COMPARATIVE ANALYSIS OF ADAPTIVE SUBBAND STRUCTURES WITH CRITICAL SAMPLING

Mariane R. Petraglia *Renata T. B. Vasconcellos*

Program of Electrical Eng., COPPE, EE - Federal University of Rio de Janeiro
CP 68504, CEP 21945-970, Rio de Janeiro, RJ - Brazil
{mariane,renatav}@lps.ufrj.br

ABSTRACT

Subband adaptive algorithms have been developed for applications such as acoustic echo cancellation and wideband active noise control, which require adaptive filters with thousands of taps resulting in high computational complexity and slow adaptation convergence. By using subband adaptive algorithms, both computational complexity and convergence rate may be reduced. Structures with non-critical sampling of the subband signals have been frequently employed in order to avoid aliasing effects. Recently, new subband structures with critical sampling have been developed in which the aliasing between adjacent subbands is completely canceled. In this paper, theoretical analyses of the convergence behaviors of subband adaptive algorithms with critical sampling are presented, from which the convergence rates and minimum mean-square errors can be estimated.

1. INTRODUCTION

Adaptive FIR filters are used in many applications, in view of their stability and unimodal performance properties. However, in some applications such as acoustic echo cancellation and wideband active noise control [1], the order of the adaptive filters is very high, resulting in a large number of operations for their implementation and slow convergence of the coefficients. To solve these problems, subband processing techniques have been proposed for the adaptive filters [2]-[4]. The advantages of subband processing are: the computational complexity is reduced by approximately the down-sampling factor, because both the number of taps and weight update rate can be decimated in each subband; and the convergence rate is improved because the spectral dynamic range is greatly reduced in each subband.

To implement the subband adaptive algorithms, oversampled subband structures [2] and critically sampled structures [3],[4] have been derived. In order to model a finite impulse response (FIR) system with small asymptotic errors, adaptive subband structures with critical sampling require additional adaptive cross filters among the subbands [3], as illustrated in Fig. 1. The separate adaptation of the direct path and cross filters results in slow convergence rate, and such approach will be referred here as overdetermined subband structure. In [4], a novel adaptive subband structure with critical sampling was derived, where the extra filters among the subbands are directly related to the direct-path adaptive filters, and do not need to be adapted separately. The resulting structure is illustrated in Fig. 2 and will be referred here as non-overdetermined subband structure.

This work was partially supported by CAPES and CNPq, Brazil.

In this paper, the behaviors of the critically sampled adaptive subband structures of Figs. 1 and 2 are analyzed and compared.

2. OVERDETERMINED SUBBAND STRUCTURE WITH CRITICAL SAMPLING

The critically sampled subband structure derived in [3] and illustrated in Fig. 1 presents cross filters between adjacents subbands in order to cancel the aliasing among adjacents subbands. The number of adaptive filters in an M channel structure is $3M-2$, and each of these subfilters have $K=(N_s+N_h+N_f)/M$ coefficients, where N_s, N_h and N_f are the lengths of the unknown system, analysis filters and synthesis filters, respectively. Denoting $\boldsymbol{G}_{k,l}(m)$ the $K\times 1$ vector containing the coefficients of the direct and cross filters which generate the kth band output signal and $\boldsymbol{X}_l(m)$ the $K\times 1$ vector containing the K most recent samples of the subband signal X_l of Fig. 1 at iteration m, the update equation for the subfilters coefficients is

$$\boldsymbol{G}_{k,l}(m+1)=\boldsymbol{G}_{k,l}(m)+\mu_k\boldsymbol{X}_l(m)E_k(m) \qquad (1)$$

for $k=0,1,\cdots,M$ and $l=k-1,k,k+1$, where

$$\begin{aligned} E_k(m) &= D_k(m-\Delta)-[\boldsymbol{X}^T_{k-1}(m)\boldsymbol{G}_{k,k-1}(m) \\ &+ \boldsymbol{X}^T_k(m)\boldsymbol{G}_{k,k}(m)+\boldsymbol{X}^T_{k+1}(m)\boldsymbol{G}_{k,k+1}(m) \end{aligned} \qquad (2)$$

$D_k(m)$ is the kth band decomposed desired signal, and $\Delta=(N_h+N_f)/2M$ corresponds to the delay introduced by the filter banks in the subband model.

2.1. Convergence Analysis

In system identification of an unknown system $S(z)$, the subband desired signals $D_k(z)=H_k(z)S(z)X(z)$ (before down-sampling and without measurement noise) can be written as:

$$\begin{bmatrix} D_0(z) \\ D_1(z) \\ \vdots \\ D_{M-1}(z) \end{bmatrix} = \boldsymbol{H}_p(z^M)\boldsymbol{S}_{pc}(z^M)\begin{bmatrix} 1 \\ z^{-1} \\ \vdots \\ z^{-(M-1)} \end{bmatrix} X(z) \qquad (3)$$

where $\boldsymbol{H}_p(z)$ is the type-1 polyphase matrix of the analysis bank and $\boldsymbol{S}_{pc}(z)$ is the pseudo-circulant matrix formed by the type-1 polyphase components $\{S_0(z),\cdots,S_{M-1}(z)\}$ of $S(z)$, i.e.,

$$\boldsymbol{S}_{pc}(z)=\begin{bmatrix} S_0(z) & S_1(z) & \cdots & S_{M-1}(z) \\ z^{-1}S_{M-1}(z) & S_0(z) & \cdots & S_{M-2}(z) \\ \vdots & \ddots & \ddots & \vdots \\ z^{-1}S_1(z) & z^{-1}S_2(z) & \cdots & S_0(z) \end{bmatrix} \qquad (4)$$

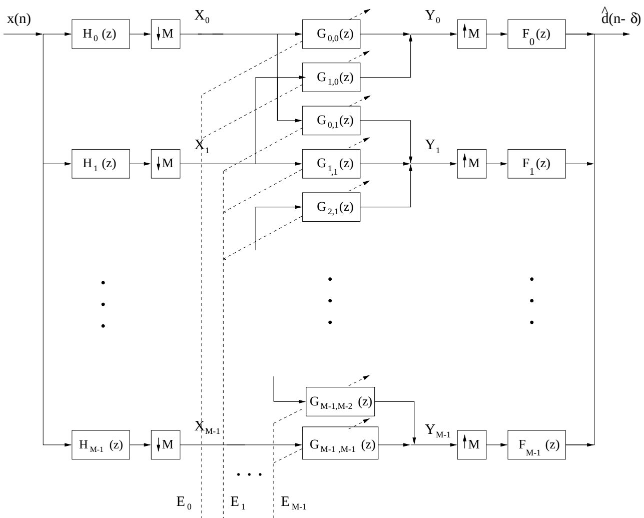

Fig. 1. Overdetermined adaptive subband structure with critical sampling [3].

In order to exactly model an arbitrary FIR system, direct-path filters and cross-filters between each two subbands are required. Denoting $\boldsymbol{C}(z)$ the $M \times M$ matrix containing the transfer functions of such filters, the subband ouput signals are given by

$$\begin{bmatrix} Y_0(z) \\ Y_1(z) \\ \vdots \\ Y_{M-1}(z) \end{bmatrix} = \boldsymbol{C}(z^M)\boldsymbol{H}_p(z^M) \begin{bmatrix} 1 \\ z^{-1} \\ \vdots \\ z^{-(M-1)} \end{bmatrix} X(z) \tag{5}$$

From (4) and (6), for exact modeling of $S(z)$, the subfilters $C_{i,j}(z)$ should be

$$\boldsymbol{C}(z) = \boldsymbol{H}_p(z)\boldsymbol{S}_{pc}(z)\boldsymbol{F}_p(z) \tag{6}$$

with $\boldsymbol{F}_p(z)$ being the type-2 polyphase matrix of the associated perfect-reconstruction synthesis bank (i.e., $\boldsymbol{H}_p(z)\boldsymbol{F}_p(z) = \boldsymbol{I}z^{-\Delta}$). Such subband modeling results in the introduction of an input-output delay Δ (inherent to the filter banks) which is taken into account by the adaptation algorithm of (2).

The decomposed desired signals (including now a measurement noise $V(k(m))$ can be expressed in terms of the optimal filters $C_{i,j}(z)$ of the subband model as

$$D_k(m-\Delta) = [\, \boldsymbol{X}_0^T(m) \ \cdots \ \boldsymbol{X}_{M-1}^T(m) \,]\boldsymbol{C}_k + V_k(m) \tag{7}$$

where $\boldsymbol{C}_k$ is the vector with the coefficients of the subfilters of the kth row of the matrix $\boldsymbol{C}(z)$ of (6).

For the subsequent stochastic analysis, we use the "independence theory" [5] and assume that the measurement noise and input signal are uncorrelated. Substituting (2) and (7) in (1), taking expected values of both sides of the resulting equation, and defining $\boldsymbol{G}_k^T(m) = [\boldsymbol{G}_{k,k-1}^T(m) \ \boldsymbol{G}_{k,k}^T(m) \ \boldsymbol{G}_{k,k+1}^T(m)]$, we obtain

$$E[\boldsymbol{G}_k(m+1)] = (\boldsymbol{I} - \mu_k \boldsymbol{R}_k)E[\boldsymbol{G}_k(m)] + \mu_k \tilde{\boldsymbol{R}}_k(m)\boldsymbol{C}_k \tag{8}$$

where

$$\boldsymbol{R}_k = \begin{bmatrix} \boldsymbol{R}_{k-1,k-1} & \boldsymbol{R}_{k-1,k} & \boldsymbol{R}_{k-1,k+1} \\ \boldsymbol{R}_{k,k-1} & \boldsymbol{R}_{k,k} & \boldsymbol{R}_{k,k+1} \\ \boldsymbol{R}_{k+1,k-1} & \boldsymbol{R}_{k+1,k} & \boldsymbol{R}_{k+1,k+1} \end{bmatrix} \tag{9}$$

$$\tilde{\boldsymbol{R}}_k = \begin{bmatrix} \boldsymbol{R}_{k-1,0} & \boldsymbol{R}_{k-1,1} & \cdots & \boldsymbol{R}_{k-1,M-1} \\ \boldsymbol{R}_{k,0} & \boldsymbol{R}_{k,1} & \cdots & \boldsymbol{R}_{k,M-1} \\ \boldsymbol{R}_{k+1,0} & \boldsymbol{R}_{k+1,1} & \cdots & \boldsymbol{R}_{k+1,M-1} \end{bmatrix} \tag{10}$$

with

$$\boldsymbol{R}_{k,l} = E[\boldsymbol{X}_k(m)\boldsymbol{X}_l^T(m)] = \boldsymbol{H}_k \boldsymbol{R}_{xx} \boldsymbol{H}_l^T \tag{11}$$

$\boldsymbol{R}_{xx}$ is the $N \times N$ input-signal autocorrelation matrix and $\boldsymbol{H}_k$ is a $K \times N$ matrix, with $N = N_h + (K-1)M$, whose first row has the N_h coefficients of $H_k(z)$ followed by $(K-1)M$ zeros, and every following row is given by the previous one circularly shifted to the right by M positions.

After convergence, $E[\boldsymbol{G}_k(m+1)] = E[\boldsymbol{G}_k(m)] = \overline{\boldsymbol{G}}_k$, and, from (8),

$$\overline{\boldsymbol{G}}_k = \boldsymbol{R}_k^{-1}\tilde{\boldsymbol{R}}_k\boldsymbol{C}_k \tag{12}$$

For white noise input and orthogonal filter banks it can be easily shown that $\boldsymbol{R}_{k,l} = \boldsymbol{0}$, for $k \neq l$, and $\boldsymbol{R}_{k,k} = \sigma_x^2\boldsymbol{I}$, and therefore, $\overline{\boldsymbol{G}}_k = [\, \boldsymbol{C}_{k,k-1}^T \ \boldsymbol{C}_{k,k}^T \ \boldsymbol{C}_{k,k+1}^T \,]$. Such result is also valid for colored inputs when the stopband attenuations of the analysis filters are large enough such that $\boldsymbol{R}_{k,l} \approx \boldsymbol{0}$ for $|k-l| > 1$. Also from (8), we observe that the convergence in the mean of the kth band adaptive coefficients is governed by the eigenvalue spread of the matrix $\boldsymbol{R}_k$.

For lossless filter banks, the total MSE is given by

$$\xi(m) = \sum_{k=0}^{M-1} E[E_k^2(m)] \tag{13}$$

Its minimum value (with the optimal coefficients $\overline{\boldsymbol{G}}_k$) is obtained substituting (2) and (7) in the above equation, i.e.,

$$\xi_{min} = \sum_{k=0}^{M-1} (\boldsymbol{C}_k^T\hat{\boldsymbol{R}}\boldsymbol{C}_k - 2\boldsymbol{C}_k^T\tilde{\boldsymbol{R}}_k\overline{\boldsymbol{G}}_k + \overline{\boldsymbol{G}}_k^T\boldsymbol{R}_k\overline{\boldsymbol{G}}_k) + \sigma_v^2 \tag{14}$$

where

$$\hat{\boldsymbol{R}} = \begin{bmatrix} \boldsymbol{R}_{0,0} & \cdots & \boldsymbol{R}_{0,M-1} \\ \vdots & \ddots & \vdots \\ \boldsymbol{R}_{M-1,0} & \cdots & \boldsymbol{R}_{M-1,M-1} \end{bmatrix} \tag{15}$$

and σ_v^2 is the measurement noise variance.

3. NON-OVERDETERMINED SUBBAND STRUCTURE WITH CRITICAL SAMPLING

The critically sampled subband structure of Fig. 2 was presented in [4]. In its derivation, it was considered that non-adjacent filters of the analysis bank had non-overlapping frequency responses. The resulting structure also presents extra filters among the subbands, but such filters are directly related to the direct-path filters, and do not need to be adapted separately. The lengths of the subfilters $G_k(z)$ should be at least $K = (N_s + N_f)/M - 1$.

Denoting $\boldsymbol{G}(m)$ the $MK \times 1$ vector containing all adaptive coefficients, i.e.,

$$\boldsymbol{G}(m) = [\, \boldsymbol{G}_0{}^T(m) \ \ \boldsymbol{G}_1{}^T(m) \ \ \ldots \ \ \boldsymbol{G}_{M-1}{}^T(m) \,]^T \tag{16}$$

$\boldsymbol{X}_{k,l}(m)$ the $K \times 1$ vector with the most recent K samples of the subband signal $X_{k,l}$ of Fig. 2, and $\boldsymbol{E}(m)$ and $\boldsymbol{D}(m)$ the $M \times 1$

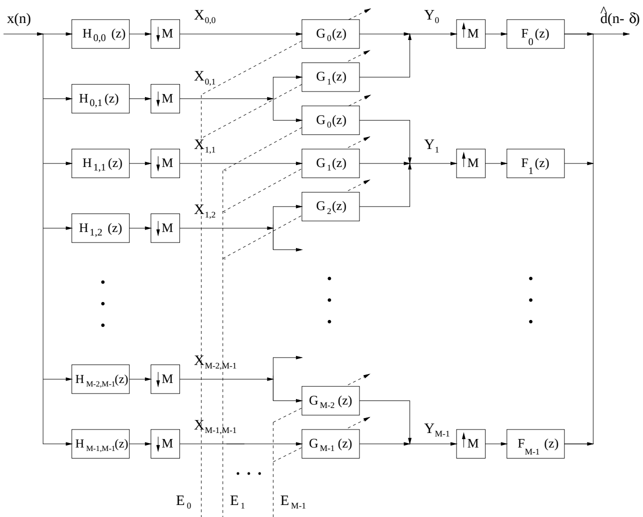

Fig. 2. Non-overdetermined adaptive subband structure with critical sampling [4].

vectors with the subband errors and desired signals, respectively, at iteration m, the coefficient update equation in vector form is [4]

$$\boldsymbol{G}(m+1) = \boldsymbol{G}(m) + \boldsymbol{\mu}\mathcal{X}(m)\boldsymbol{E}(m) \tag{17}$$

where $\boldsymbol{\mu} = \mathrm{diag}\{\mu_0\boldsymbol{I}_K, \mu_1\boldsymbol{I}_K, \cdots, \mu_{M-1}\boldsymbol{I}_K\}$,

$$\mathcal{X}(m) = \begin{bmatrix} \boldsymbol{X}_{0,0} & \boldsymbol{X}_{0,1} & & & \\ \boldsymbol{X}_{1,0} & \boldsymbol{X}_{1,1} & \boldsymbol{X}_{1,2} & & \\ & \ddots & \ddots & \ddots & \\ & & & \boldsymbol{X}_{M-1,M-2} & \boldsymbol{X}_{M-1,M-1} \end{bmatrix} \tag{18}$$

and

$$\boldsymbol{E}(m) = \boldsymbol{D}(m-\Delta) - \mathcal{X}^T(m)\boldsymbol{G}(m) \tag{19}$$

with $\Delta = (N_h + N_f)/2M - 2$.

3.1. Convergence Analysis

Applying the generalized subband decomposition [4] to the unknown system, we can write

$$S(z) = z^{\Delta M}\left[\, \hat{G}_0(z^M) \;\cdots\; \hat{G}_{M-1}(z^M) \,\right] \boldsymbol{H}_p(z^M) \begin{bmatrix} 1 \\ z^{-1} \\ \vdots \\ z^{-(M-1)} \end{bmatrix} \tag{20}$$

where

$$\left[\, \hat{G}_0(z) \;\cdots\; \hat{G}_{M-1}(z) \,\right] = \left[\, S_0(z) \;\cdots\; S_{M-1}(z) \,\right] \boldsymbol{F}_p(z) \tag{21}$$

with $S_i(z)$ and $\boldsymbol{F}_p(z)$ as defined in Section 2. Thus, denoting $\hat{\boldsymbol{G}}$ the vector with the coefficients of $\hat{G}_0(z), \cdots, \hat{G}_{M-1}(z)$, the subband desired signals can be written as

$$\boldsymbol{D}(m-\Delta) = \hat{\mathcal{X}}^T(m)\hat{\boldsymbol{G}} + \boldsymbol{V}(m) \tag{22}$$

where

$$\hat{\mathcal{X}}(m) = \begin{bmatrix} \boldsymbol{X}_{0,0}(m) & \cdots & \boldsymbol{X}_{0,M-1}(m) \\ \vdots & \ddots & \vdots \\ \boldsymbol{X}_{M-1,0}(m) & \cdots & \boldsymbol{X}_{M-1,M-1}(m) \end{bmatrix} \tag{23}$$

and $\boldsymbol{V}(m)$ contains the subband measurement errors.

Then, substituting (19) and (22) in (17) and taking expected values of both sides of the resulting equation, we obtain

$$E[\boldsymbol{G}(m+1)] = (\boldsymbol{I} - \boldsymbol{\mu}\mathcal{R})E[\boldsymbol{G}(m)] + \boldsymbol{\mu}\tilde{\mathcal{R}}\hat{\boldsymbol{G}} \tag{24}$$

where $\mathcal{R} = E[\mathcal{X}(m)\mathcal{X}^T(m)]$ and $\tilde{\mathcal{R}} = E[\mathcal{X}(m)\hat{\mathcal{X}}^T(m)]$. The matrices $\mathcal{R}$ and $\tilde{\mathcal{R}}$ can be expressed in terms of the input signal and of the analysis filters coefficients, since their submatrices are

$$E[\boldsymbol{X}_{k,l}\boldsymbol{X}_{m,n}^T] = \boldsymbol{H}_{k,l}\boldsymbol{R}_{xx}\boldsymbol{H}_{m,n}^T \tag{25}$$

where $\boldsymbol{H}_{k,l}$ is an $N \times K$ matrix, with $N = 2N_h - 1 + M(K-1)$, formed as $\boldsymbol{H}_k$ of (11) but with the coefficients of $H_k(z)H_l(z)$.

From (24), the convergence rate of the mean adaptive coefficients is determined by the eigenvalue ratio of the matrix $\boldsymbol{\mu}\mathcal{R}$. After convergence, $E[\boldsymbol{G}(m+1)] = E[\boldsymbol{G}(m)] = \overline{\boldsymbol{G}}$, and

$$\overline{\boldsymbol{G}} = \mathcal{R}^{-1}\,\tilde{\mathcal{R}}\hat{\boldsymbol{G}} \tag{26}$$

As the stopband attenuation of the analysis filters increases, $\tilde{\mathcal{R}} \approx \mathcal{R}$ (since $E[\boldsymbol{X}_{i,j}\boldsymbol{X}_{k,l}^T] \approx \boldsymbol{0}$ for $|k-i| > 1$ and $|l-j| > 1$) and, from the above expression, $\overline{\boldsymbol{G}} \approx \hat{\boldsymbol{G}}$.

Considering lossless filter banks, using the optimal coefficients $\overline{\boldsymbol{G}}$ and Eqs. (19) and (22) in (13), the minimum MSE for the structure of Fig. 2 is given by

$$\xi_{min} = \overline{\boldsymbol{G}}^T\mathcal{R}\overline{\boldsymbol{G}} - 2\hat{\boldsymbol{G}}^T\tilde{\mathcal{R}}\overline{\boldsymbol{G}} + \hat{\boldsymbol{G}}^T\hat{\mathcal{R}}\hat{\boldsymbol{G}} + \sigma_v^2 \tag{27}$$

where $\hat{\mathcal{R}} = E[\hat{\mathcal{X}}(m)\hat{\mathcal{X}}^T(m)]$. For selective analysis filters such that $E[\boldsymbol{G}(\infty)] \approx \hat{\boldsymbol{G}}$, we obtain

$$\xi_{min} \approx \hat{\boldsymbol{G}}^T\boldsymbol{\Phi}\hat{\boldsymbol{G}} + \sigma_v^2 \tag{28}$$

where

$$\boldsymbol{\Phi} \;=\; E[(\hat{\mathcal{X}}(m) - \mathcal{X}(m))(\hat{\mathcal{X}}(m) - \mathcal{X}^T(m))] \tag{29}$$

From (28), the minimum MSE of the subband structure of Fig. 2 will be, in general, larger than the measurement noise variance σ_v^2, because of the residual aliasing not canceled in the simplified structure. The corresponding increase in the minimum MSE is related to the stopband attenuation of the analysis filters, since the matrix $\boldsymbol{\Phi}$ in (29) contains the cross-correlation matrices of non-adjacent subband signals.

4. SIMULATION RESULTS

The identification of a length $N_s = 128$ FIR system (with coefficients randomly generated) is considered, with both white and colored input signals. The colored noise was produced by passing a white noise sequence by a first-order IIR filter with pole located at $z = 0.9$. No measurement noise was added to the desired signal (i.e., $\sigma_v^2 = 0$). The adaptive structures of Figs. 1 and 2 were simulated with $M = 4$ subbands, employing cosine modulated filter banks with near-perfect reconstruction prototype filters [6] of

Table 1. Theoretical and experimental MSEs (in dB) for the overdetermined subband structure of Fig. 1

	white noise		colored noise	
N_h	16	32	16	32
ξ_{min}	-32.56	-47.62	-32.23	-47.45
ξ_{exp}	-28.24	-44.53	-29.59	-45.21

Table 2. Theoretical and experimental MSEs (in dB) for the non-overdetermined subband structure of Fig. 2

	white noise		colored noise	
N_h	16	32	16	32
ξ_{min}	-31.81	-47.83	-34.75	-49.28
ξ_{exp}	-30.73	-46.70	-31.83	-47.64

lengths $N_h = 16$ and $N_h = 32$. The theoretical minimum MSE (ξ_{min}, Eq. (14)) as well as the experimental MSE (ξ_{exp}) obtained with the structure of Fig. 1 with the two prototype filters are given in Table 1. The corresponding theoretical ξ_{min} (Eq. (28)) and ξ_{exp} for the structure of Fig. 2 are given in Table 2. Figures 3 and 4 present the mean-square error (MSE) evolutions of the subband structures of Figs. 1 and 2, respectively, for the colored input.

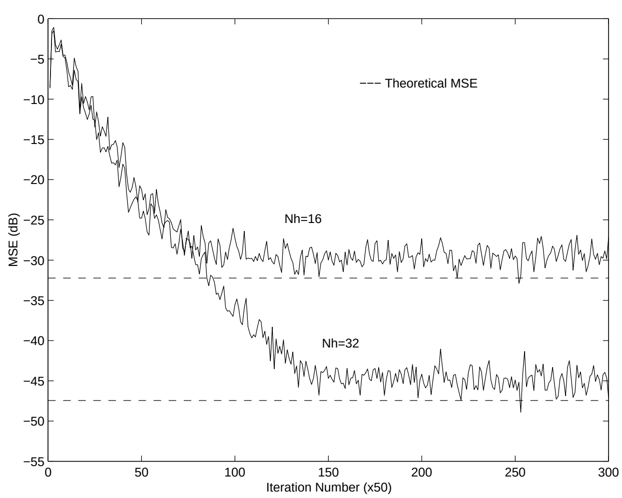

Fig. 3. MSE evolution of the overdetermined subband structure of Fig. 1 with colored input.

The eigenvalue spread of the corresponding theoretical correlation matrices for the simulations of Figs. 3 and 4 are given in Table 3. We observe from Tables 1 and 2 and from Figs. 3 and 4 that the theoretical mean-square errors are in good agreement with the experimental values and, therefore, with some knowledge of the input signal statistics, one can predict the final mean-square error of the structures for a chosen filter bank. The convergence rates of the subband algorithms can also be predicted from the analysis, as shown in Table 3 for the experiments of Figs. 3 and 4.

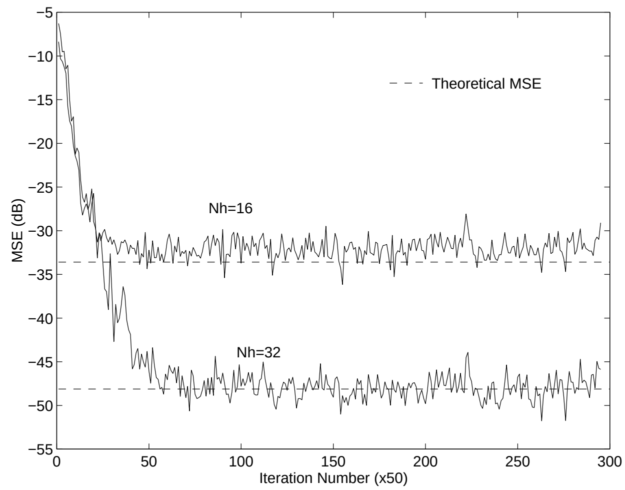

Fig. 4. MSE evolution of the non-overdetermined subband structure of Fig. 2 with colored input.

Table 3. Eigenvalue spread of the corresponding correlation matrices for the simulations of Fig. 3 and Fig. 4

	Overdetermined Str.		Non-overdet. Str.	
N_h	16	32	16	32
$\lambda_{max}/\lambda_{min}$	50.19	51.27	12.48	18.27

5. CONCLUSION

This paper provides an improved understanding of the convergence properties of recently proposed subband adaptive algorithms with critical sampling. Theoretical expressions for the mean coefficient vector and minimum mean-square errors have been derived, with the residual aliasing in the subband structures taken into account.

6. REFERENCES

[1] C. Breining *et al.*, “Acoustic Echo Control,” *IEEE Signal Processing Magazine*, pp. 42-69, Jul. 1999.

[2] W. Kellermann, “Analysis and design of multirate systems for cancellation of acoustical echoes,” *Proc. IEEE Int. Conf. Acoust., Speech, Sig. Proc.*, pp. 2570-2573, New York, NY, Apr. 1988.

[3] A. Gilloire and M. Vetterli, “Adaptive filtering in subbands with critical sampling: analysis, experiments, and application to acoustic echo cancellation,” *IEEE Trans. Signal Processing*, pp. 1862-1875, vol. 40, no. 8, Aug. 1992.

[4] M. R. Petraglia, R. G. Alves and P. S. R. Diniz, “New Structures for Adaptive in Subbands with Critical Sampling,” *IEEE Trans. on Signal Processing*, vol. 48, No. 12, pp. 3316-3327, Dec. 2000.

[5] S. Haykin, *Adaptive Filter Theory*, 3rd ed., Prentice-Hall, Englewood Cliffs, New Jersey, 1996.

[6] G. Strang and T. Nguyen, *Wavelets and Filter Banks*. Wellesley - Cambridge Press, 1996.